J|A|C|S ARTICLES

Published on Web 05/06/2010

Mechanistic Insights into Alkene Epoxidation with H_2O_2 by Ti- and other TM-Containing Polyoxometalates: Role of the Metal Nature and Coordination Environment

Nadya S. Antonova,[†] Jorge J. Carbó,*[,†] Ulrich Kortz,[‡] Oxana A. Kholdeeva,[§] and Josep M. Poblet*[,†]

Department de Química Física i Inorgànica, Universitat Rovira i Vigili, Marcel·lí Domingo s/n, 43007 Tarragona, Spain, School of Engineering and Science, Jacobs University, P.O. Box 750561, 28725 Bremen, Germany, and Boreskov Institute of Catalysis, Russian Academy of Sciences, Lavrentiev Avenue 5, Novorsibirsk 630090, Russia

Received March 19, 2010; E-mail: j.carbo@urv.cat; josepmaria.poblet@urv.cat

Abstract: The oxidation of alkenes by H_2O_2 catalyzed by Ti(IV)-containing polyoxometalates (POMs) as models of Ti single-site catalysts has been investigated at DFT level and has been compared with other early transition-metal-substituted polyoxometalates. We have studied in detail the reaction mechanism of the C_2H_4 epoxidation with H_2O_2 mediated by two different POMs, the Ti-monosubstituted Keggin-type POM $[PTi(OH)W_{11}O_{39}]^{4-}$ and the Ti-disubstituted sandwich-type POM $[Ti_2(OH)_2As_2W_{19}O_{67}(H_2O)]^{8-}$. These species exhibit well-defined 6- and 5-coordinated titanium environments. For both species, the reaction proceeds through a two-step mechanism: (i) the Ti-OH groups activate H_2O_2 with a moderate energy barrier yielding either Ti-hydroperoxo (Ti^{IV}-OOH) or Ti-peroxo (Ti^{IV}-OO) intermediate, and (ii) the less stable but more reactive Ti-hydroperoxo species transfers oxygen to alkene to form the epoxide, this latter step being the rate-determining step. The higher activity of the sandwich anion was attributed to the absence of dimer formation, and its higher selectivity to the larger energy cost of homolytic O−O bond breaking in the hydroperoxo intermediate. We also propose several requisites to improve the efficiency of Ti-containing catalysts, including flexible and 5-fold (or lower) coordinated Ti environments, as well as reagent-accessible Ti sites. Calculations on other TM-containing Keggin-type POMs $[PTM(OH)W_{11}O_{39}]^{4-}$ (TM = Zr(IV), V(V), Nb(V), Mo(VI), W(VI), and Re(VII)) showed that when we move from the left to the right in the periodic table the formation of the epoxide via peroxo intermediate becomes competitive because of the higher mixing between the orbitals of the TM and the O−O unit.

Introduction

Alkene epoxidation is one of the fundamental reactions in organic synthesis because epoxides are used as key intermediates for the manufacture of a wide variety of valuable products.[1,2] The development and implementation of catalytic processes for selective alkene epoxidation, which eliminate the use of hazardous reactants and reduce generation of waste, is an important goal.[2] Hydrogen peroxide is quite cheap and readily available and gives water as the only co-product. All of these qualities make it an attractive environmentally friendly oxidant.[2,3] Titanium-containing catalysts have attracted great attention due to their ability to activate hydrogen peroxide.[4] The discovery of the microporous titanium-silicalite TS-1 in the early 1980s, initiated a large family of the so-called Ti single-site catalysts.[4a,5] TS-1 possesses a unique ability to activate H_2O_2 and oxidize small organic substrates (<0.6 nm) via heterolytic oxidation mechanisms.[4c,6] To meet the demands of fine chemicals industry, many research groups have been working on the development of a mesoporous analogue of TS-1, which could be used for

[†] Universitat Rovira i Vigili.
[‡] Jacobs University.
[§] Russian Academy of Sciences.

(1) (a) Franz, G.; Sheldon, R. A. In *Ulmann's Encyclopedia of Industrial Chemistry*, 5th ed.; VCH: Weinheim, 1991; Vol. A(18), pp 261−311. (b) *Kirk-Othmer Encyclopedia of Chemical Technology*; Interscience: New York, 1985; Vol. 7, pp 239−263. (c) Sienel, G.; Rieth, R.; Rowbottom, K. T. In *Ulmann's Encyclopedia of Organic Chemicals*; Wiley-VCH: Weinheim, 1985; Vol. A(9), pp 531−545. (d) Jorgensen, K. A. *Chem. Rev.* **1989**, *89*, 432–458. (e) Dusi, M.; Mallat, T.; Baiker, A. *Catal. Rev.-Sci. Eng.* **2000**, *42*, 213–278. (f) Lane, B. S.; Burgess, K. *Chem. Rev.* **2003**, *103*, 2457–2473.

(2) (a) Sheldon, R. A.; van Vliet, M. C. A. In *Fine Chemicals through Heterogeneous Catalysis*; Sheldon, R. A., van Bekkum, H., Eds.; Wiley: Weinheim, 2001; pp 473−490. (b) Cavani, F.; Gaffney, A. M. In *Sustainable Industrial Processes*; Cavani, F., Centi, G. , Perathoner, S., Trifirò, F., Eds.; Wiley-VCH: Weinheim, 2009.

(3) (a) *Catalytic Oxidations with Hydrogen Peroxide as Oxidant*; Strukul, G., Ed.; Kluwer Academic: Dordrecht, The Netherlands, 1992. (b) Jones, C. W. *Application of Hydrogen peroxide and Derivatives*; Royal Chemical Society of Chemistry: Cambridge, 1999. (c) Sanderson, W. R. *Pure Appl. Chem.* **2000**, *72*, 1289–1304. (d) Centi, G.; Perathoner, S.; Abate, S. In *Modern Heterogeneous Oxidation Catalysis: Design, Reactions and Characterization*; Mizuno, N., Ed.; Wiley-VCH: Weinheim, 2009; pp 253−288.

(4) For selected reviews on Ti catalysts, see: (a) Notari, B. *Adv. Catal.* **1996**, *41*, 253–334. (b) Thomas, J. M.; Raja, R. *Top. Catal.* **2006**, *40*, 3–17. (c) Ratnasamy, P.; Srinivas, D.; Knozinger, H. *Adv. Catal.* **2004**, *48*, 1–169. (d) Kholdeeva, O. A.; Trukhan, N. N. *Russ. Chem. Rev.* **2006**, *75*, 411–432.

(5) (a) Taramasso, M.; Perego, G.; Notari, B. U.S. Patent 4,410,501, 1983. (b) Clerici, M. G. *Top. Catal.* **2000**, *13*, 373–386. Perego, C.; Carati, A.; Ingalina, P.; Mantegazza, M. A.; Bellussi, G. *Appl. Catal., A* **2001**, *221*, 63–72.

 10.1021/ja1023157

H_2O_2-based oxidation of large organic molecules.[7] However, the majority of mesoporous titanium-silicates revealed a catalytic behavior, which differed from TS-1 by a significant contribution of homolytic oxidation routes.[4c] To date, the reasons for that are not completely understood and remain under debate.

Homogeneous catalysts are often tractable and suitable for probing interactions at the molecular level. Therefore, studies on soluble titanium compounds with different structures might shed light on the mechanisms of H_2O_2 activation by different kinds of Ti centers. Titanium-substituted polyoxometalates (POMs for short) have inorganic nature, are thermodynamically stable to oxidation, and possess hydrolytic stability under appropriate pH conditions, which makes them suitable molecular models for Ti centers in aqueous−organic media.[8] The apparent structural analogy of POMs and metal oxide surfaces allows one to view POMs as discrete, soluble fragments of extended metal oxide lattices.[9] Recently, Kholdeeva et al. have demonstrated that the catalytic performance of the salt $[TBA]_4[PTi(OH)W_{11}O_{39}]$ (**1a**) in the oxidation of alkenes, thioethers, and alkylphenols with H_2O_2 is very similar to the performance of hydrophilic mesoporous titanium-silicates.[8,10] In **1a**, the $PW_{11}O_{39}^{7-}$ lacunary species acts as a pentadentate ligand for the hexa-coordinated Ti(IV) ion. Thus, only one external coordination position is labile and participates in interactions with reactants in the course of an oxidation process. Also, the oxygen sites linked to the Ti center are always the most basic.[11] It has been established that such hexa-coordinated isolated Ti centers catalyze oxidation reactions with H_2O_2 predominantly via homolytic oxidation routes.[8]

Recently, "sandwich"-type dititanium 19-tungstodiarsenate(III) $[Ti_2(OH)_2As_2W_{19}O_{67}(H_2O)]^{8-}$ (**1b**) (the structure is shown in Figure 1) has been synthesized and characterized by single-crystal X-ray diffractometry, IR, TGA/DSC, electrochemistry, and elemental analysis.[12a]

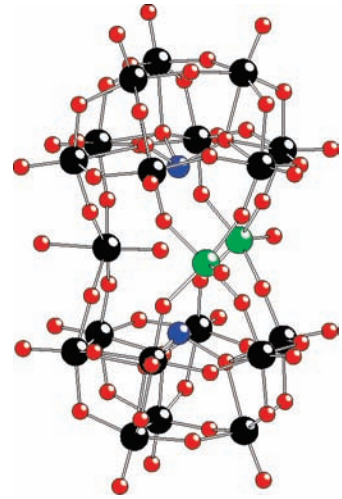

Figure 1. Ball-and-stick representation of polyanion **1b**.

Polyanion **1b** comprises two (B-α-$As^{III}W_9O_{33}$) Keggin moieties linked via two square-pyramidal $[Ti(OH)]^{3+}$ groups and an octahedral $[WO(H_2O)]^{4+}$ fragment. The unprecedented arrangement of the two TiOH groups in **1b** allows neither *intra*- nor *inter*-molecular Ti−O−Ti bond formation. Following our interest in Ti-containing soluble probes and keeping in mind the unusual coordination environment of Ti in polyanion **1b**, we explored the catalytic properties of **1b** in the selective oxidation of a range of organic compounds with H_2O_2.[12] Surprisingly, **1b** appeared to be highly active and selective in the latter reaction, leading to products typical of a heterolytic oxidation mechanism. To clarify the role titanium atoms in **1b**, a comparison with the Ti-free analogue $[As_2W_{21}O_{67}(H_2O)]^{6-}$ and monosubstituted Keggin (**1a**) and other multi-Ti-center POMs (Ti_n-POM) was made, and the stability of **1b** under turnover conditions was verified.[12b] The Ti-free analogue of **1b** with only W atoms in the belt was found to be completely inactive in cyclohexene oxidation,[12b] which indicates that the presence of Ti is crucial for this reaction. Ti-POMs having hexa-coordinated Ti atoms turned out to be highly active in nonproductive decomposition of hydrogen peroxide and, in the presence of cyclohexene, produced allylic oxidation products 2-cyclohexene-1-ol and 2-cyclohexene-1-one, along with epoxide and diol.

The mechanism of titanium(IV)-based oxidation has been extensively studied.[13−27] For titanosilicate-type catalysts, the addition of hydrogen peroxide can yield the titanium-hydroperoxo (TiOOH) and the titanium-peroxo (TiOO) species.[13] It is generally agreed that titanium-hydroperoxo groups are the active oxygen-donating intermediates for the epoxidation of alkenes.[16−24] Alternatively, mechanisms without Ti-OOH or Ti-OO formation

(6) Clerici, M. G. In *Proceedings of the DGMK/SCI Conference: Oxidation and Functionalisation: Classical and Alternative Routes and Sources*; DGMK: Hamburg, 2005; pp 165−176.
(7) (a) Tanev, P. T.; Chibwe, M.; Pinnavaia, T. J. *Nature* **1994**, *368*, 321–323. (b) Corma, A.; Domine, M.; Gaona, J. A.; Jorda, J. L.; Navarro, M. T.; Rey, F.; Perez-Pariente, J.; Tsuji, J.; McCulloch, B.; Neneth, L. T. *Chem. Commun.* **1998**, 2211–2212. (c) Fraile, J. M.; Garcia, J. I.; Mayoral, J. A.; Vispe, E. *J. Catal.* **2000**, *189*, 40–51. (d) Bhaumik, A.; Tatsumi, T. *J. Catal.* **2000**, *189*, 31–39. (e) Shan, Z.; Jansen, J. C.; Marchese, L.; Maschmeyer, T. *Microporous Mesoporous Mater.* **2001**, *48*, 181–187. (f) Guidotti, M.; Ravasio, N.; Psaro, R.; Gianotti, E.; Coluccia, S; Marchese, L. *J. Mol. Catal. A: Chem.* **2006**, *250*, 218–225. (g) Barrio, L.; Campos-Martirn, J. M.; Pilar de Frutos-Escrig, M.; Fierro, J. L.G. *Microporous Mesoporous Mater.* **2008**, *113*, 542–553.
(8) (a) Kholdeeva, O. A. *Top. Catal.* **2006**, *40*, 229–243. (b) Kholdeeva, O. A.; Maksimovskaya, R. I. *J. Mol. Catal. A: Chemical* **2007**, *262*, 7–24.
(9) (a) Day, V. W.; Klemperer, W. G. *Science* **1985**, *228*, 533–541. (b) Finke, R. G.; Droege, M. W. *J. Am. Chem. Soc.* **1984**, *106*, 7274–7277. (c) Fournier, M.; Louis, C.; Che, M.; Chaquin, P.; Masure, D. *J. Catal.* **1989**, *119*, 400–414. (d) Pope, M. T.; Müller, A. *Angew. Chem., Int. Ed* **1991**, *30*, 34–48. (e) Chen, Q.; Zubieta, J. *Coord. Chem. Rev.* **1992**, *114*, 107–167.
(10) (a) Kholdeeva, O. A.; Maksimov, G. M.; Maksimovskaya, R. I.; Kovaleva, L. A.; Fedotov, M. A.; Grigoriev, V. A.; Hill, C. L. *Inorg. Chem.* **2000**, *39*, 3828–3837. (b) Kholdeeva, O. A.; Trubitsina, T. A.; Maksimovskaya, R. I.; Golovin, A. V.; Neiwert, W. A.; Kolesov, B. A.; López, X.; Poblet, J.-M. *Inorg. Chem.* **2004**, *43*, 2284–2292. (c) Kholdeeva, O. A.; Trubitsina, T. A.; Maksimov, G. M.; Golovin, A. V.; Maksimovskaya, R. I. *Inorg. Chem.* **2005**, *44*, 1635–1642. (d) Kholdeeva, O. A.; Kovaleva, L. A.; Maksimovskaya, R. I.; Maksimov, G. M. *J. Mol. Catal. A: Chem.* **2000**, 223–229.
(11) (a) Fernández, J. A.; López, X.; Poblet, J. M. *J. Mol. Catal. A: Chem.* **2007**, *262*, 236–242. (b) López, X.; Weinstock, I.; Bo, C.; Sarasa, J. P.; Poblet, J. M. *Inorg. Chem.* **2006**, *45*, 6467–6473.
(12) (a) Hussain, F.; Bassil, B. S.; Kortz, U.; Kholdeeva, O. A.; Timofeeva, M. N.; de Oliveira, P.; Keita, B.; Nadjo, L. *Chem.—Eur. J.* **2007**, *13*, 4733–4742. (b) Kholdeeva, O. A.; Donoeva, B. G.; Trubitsina, T. A.; Al-Kadamany, G.; Kortz, U. *Eur. J. Inorg. Chem.* **2009**, 5134–5141.
(13) Bordiga, S.; Bonino, F.; Damin, A.; Lamberti, C. *Phys. Chem. Chem. Phys.* **2007**, *9*, 4854–4878, and references therein.
(14) Zhidomirov, G. M.; Yakovlev, A. L.; Milov, M. A.; Kachurovskaya, N. A.; Yudanov, I. V. *Catal. Today* **1999**, *51*, 397–410.
(15) Murugavel, R.; Roesky, H. W. *Angew. Chem., Int. Ed. Engl.* **1997**, *36*, 477–479.
(16) Clerici, M. G. *Appl. Catal.* **1991**, *68*, 249–261.
(17) Karlsen, E.; Schöffel, K. *Catal. Today* **1996**, *32*, 107–114.
(18) Tantanak, D.; Vincent, M. A.; Hilier, I. H. *Chem. Commun.* **1998**, 1031–1032.

Scheme 1

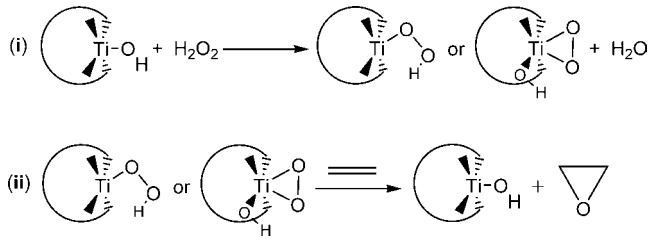

have been also proposed. Hence, Vayssilov and van Santen have proposed that the preadsorved complex of H_2O_2 on a Ti active site of TS-1 catalysts is sufficiently activated for oxygen transfer to the incoming alkene double bond.[25] However, more recent computational studies have shown that the mechanism through Ti-OOH has a lower energy barrier, at least for external surface sites.[24] Panas and co-workers have proposed a competing direct path for titanium oxides, in which there is a cooperative effect of binuclear Ti(IV) dihydroxide sites polarizing the hydrogen peroxide and favoring the oxygen transfer to the alkene.[27]

For mono- and dititanium-substituted POMs, the two latter mechanisms are unlikely: first, the Ti(IV) center occupies an *external* site, and second, as we will discuss in more detail below, the two Ti(IV) centers in **1b** are far enough from each other to discard a cooperative effect. Moreover, recent experimental studies have shown that the reaction of **1a** with H_2O_2 in MeCN affords the protonated titanium peroxo complex $[Bu_4N]_4[HPTi(O_2)W_{11}O_{39}]$.[10c] However, it is still unclear the overall picture of the reaction mechanism and whether the dititanium POM follows the same mechanism. Also, for the heterolytic mechanism, it is unknown the precise nature of the active species, i.e., whether the protonated peroxo is responsible for oxygen transfer or evolves to hydroperoxo species to form a more reactive species. On the basis of previous data, we initially examine a mechanism, which can be divided into the following two main steps (see Scheme 1): (i) the activation of H_2O_2 to form the titanium-peroxo or -hydroperxo intertemediate, and (ii) the alkene attack on the reactive intermediate to form the epoxide and water.

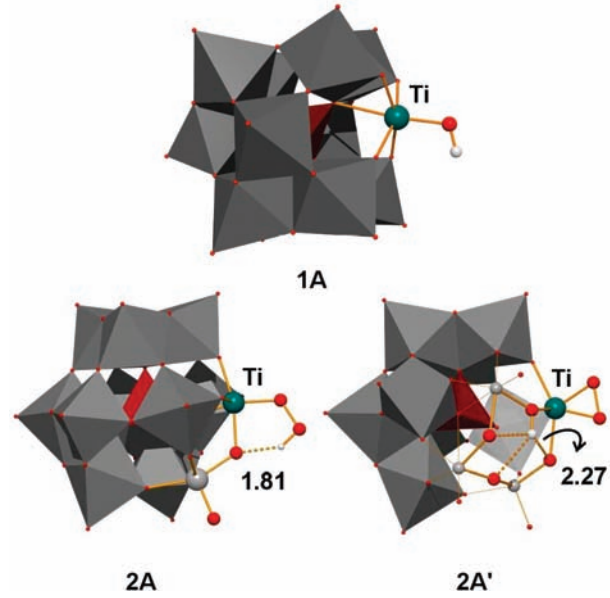

Figure 2. Structures and main distances (in Å) for Keggin-type Ti-hydroperoxo **2A** and Ti-peroxo **2A′** anions.

In the present paper, we report a detailed theoretical investigation on alkene epoxidation with hydrogen peroxide catalyzed by the Keggin monosubstituted $[PTi(OH)W_{11}O_{39}]^{4-}$ anion and the more recently discovered sandwich-like $[Ti_2(OH)_2As_2W_{19}O_{67}(H_2O)]^{8-}$ anion. For sake of comparison, we also analyze other early transition-metal-substituted POMs.

Results and Discussion

Activation of H_2O_2 by Ti-Monosubstituted Keggin Anion. To investigate the epoxidation of alkenes with hydrogen peroxide catalyzed by titanium-substituted POMs at a molecular level, we carried out density functional theory (DFT) calculations on the anions $[PTi(OH)W_{11}O_{39}]^{4-}$ (**1A**) and $[Ti_2(OH)_2As_2W_{19}O_{67}]^{8-}$ (**1B**), using ethene as the simplest alkene model. Our previous DFT study on Keggin-type $[HPTi(O_2)W_{11}O_{39}]^{4-}$ anion[10b] showed that the most stable isomer is formed preferentially after protonation of the Ti−O−W site; however the TiOO-H complex resulting from protonation of the peroxo ligand could also coexist in solution.[10b] Thus, first we recomputed the most stable isomers for titanium hydroperoxo (**2A**) and the protonated peroxo (**2A′**) POMs (Figure 2) at the B3LYP level, which has been successfully applied to reactivity studies on titanium model complexes,[19,22,23,26,27] on other substituted POMs,[28b,29] and on the other synthesized molecular models of titanium oxide.[30] In **2A** the Ti hydroperoxo moiety forms a five-membered ring via hydrogen bonding of the hydroperoxo group with the bridging Ti−O−W oxygen. In **2A′**, the peroxo moiety is η^2-coordinated and the hydrogen is oriented toward the center of the nearest M_4O_4 ring. Structure **2A** is 1.4 kcal·mol^{-1} above **2A′** in the gas phase. The energy difference reduces to 0.7 kcal·mol^{-1} if MeCN solvent ($\Gamma = 36.64$) is included in the calculations via

(19) (a) Yudanov, I. V.; Gisdakis, P.; Di Valentin, C.; Rösch, N. *Eur. J. Inorg. Chem.* **1999**, 2135–2145. (b) Rösch, N.; Di Valentin, C.; Yudanov, I. V. *Mechanism of Olefin Epoxidation by Transition Metal Peroxo Compounds in Computational Modeling of Homogenous Catalysis*; Maseras, F., Lledós, A., Eds.; Kluwer Academic Publishers: Dordrecht, 2002.
(20) (a) Sinclair, P. E.; Catlow, C. R. A. *J. Phys. Chem. B* **1999**, *103*, 1084–1095. (b) Barker, C. M.; Kaltsoyannis, N.; Catlow, C. R. A. *Stud. Surf. Sci. Catal.* **2001**, *135*, 2580–2587.
(21) Munakata, H.; Oumi, Y.; Miyamoto, A. *J. Phys. Chem. B* **2001**, *105*, 3493–3501.
(22) Kudo, T.; Gordon, M. S. *J. Phys. Chem. A* **2003**, *17*, 8756–8762.
(23) (a) Server, R. R.; Root, T. W. *J. Phys. Chem. B* **2003**, *107*, 4080–4089. (b) Server, R. R.; Root, T. W. *J. Phys. Chem. B* **2003**, *107*, 4090–4099. (c) Server, R. R.; Root, T. W. *J. Phys. Chem. B* **2003**, *107*, 10521–10530.
(24) (a) Wells, D. H.; Delgass, W. N.; Thomson, K. T *J. Am. Chem. Soc.* **2004**, *126*, 2956–2962. (b) Wells, D. H.; Joshi, A. M.; Delgass, W. N.; Thomson, K. T. *J. Phys. Chem. B* **2006**, *110*, 14627–14639.
(25) Vayssilov, G. N.; van Santen, R. A. *J. Catal.* **1998**, *175*, 170–174.
(26) Stare, J.; Henson, N. J.; Eckert, J. *J. Chem. Inf. Model.* **2009**, *49*, 833–846.
(27) (a) Lundin, A.; Panas, I.; Ahlberg, E. *Phys. Chem. Chem. Phys.* **2007**, *9*, 5997–6003. (b) Lundin, A.; Panas, I.; Ahlberg, E. *J. Phys. Chem. A* **2009**, *113*, 282–290.
(28) (a) Prabhakar, R.; Morokuma, K.; Hill, C. L.; Musaev, D. G. *Inorg. Chem.* **2006**, *45*, 5703–5709. (b) Kuznetsov, A. E.; Geletii, Y. V.; Hill, C. L.; Morokuma, K.; Musaev, D. G. *Inorg. Chem.* **2009**, *48*, 1871–1878.
(29) (a) Nakagawa, Y.; Mizuno, N. *Inorg. Chem.* **2007**, *46*, 1727–1736. (b) Kamata, K.; Hirano, T.; Kuzuya, S.; Mizuno, N. *J. Am. Chem. Soc.* **2009**, *131*, 6997–7004.
(30) (a) Carbó, J. J.; González-del Moral, O.; Martín, A.; Mena, M.; Poblet, J.-M.; Santamaría, C. *Chem.—Eur. J.* **2008**, *14*, 7930–7938. (b) Carbó, J. J.; González-del-Moral, O.; Martín, A.; Mena, M.; Poblet, J. M.; Santamaría, C. *Eur. J. Inorg. Chem.* **2009**, 643–653.

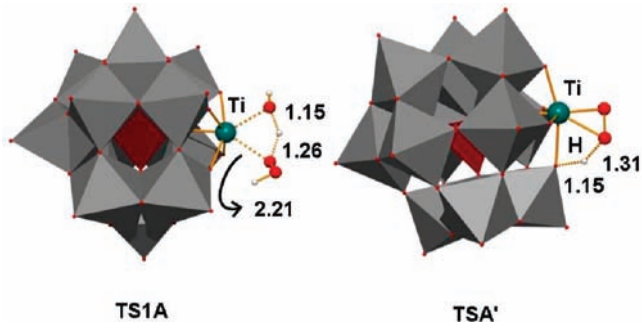

Figure 3. Transition state structures and main distances (in Å) for the H_2O_2 activation (**TS1A**) and the proton transfer between the hydroperoxo and protonated peroxo species (**TSA′**) in Ti-monosubstituted Keggin anion.

a continuum model.[31] Therefore, the present calculations do also predict that the side-on η^2 Ti-peroxo complex **2A′** is more stable than the end-on η^1 Ti-hydroperoxo **2A** but in only a small energy amount, which does not preclude the coexistence of both species.

In a step forward, we analyze the formation and interconversion of hydroperoxo (**2A**) and peroxo (**2A′**) structures. Figure 3 collects the geometries of the transition states involved in the processes. The formation of **2A** and **2A′** from the hydroxo complex **1A** and H_2O_2 is computed to be exothermic by 5.8 and 7.1 kcal·mol^{-1}, respectively. The computed exothermicity in the gas phase agrees qualitatively with the determined equilibrium constant ($K_1 = 10$), which indicates that the reaction of $[Bu_4N]_4$ $[PTi(OH)W_{11}O_{39}]$ with H_2O_2 to yield $[Bu_4N]_4$-$[HPTi(O_2)W_{11}O_{39}]$ and H_2O is displaced to products.[10c] Nevertheless, assuming a Boltzmann distribution between reactants and products, we estimate a reaction energy of −1.7 kcal·mol^{-1} from the equilibrium constant. Thus, we must conclude that the computed values in vacuum (−5.8 and −7.1 kcal·mol^{-1}) overestimate the exothermicity of the reaction.

To attempt to improve our results, we initially include the solvent effects via the continuum IEF-PCM model.[31] The relative energies for **2A** and **2A′** change, respectively, from −5.8 and −7.1 kcal·mol^{-1} in vacuum to +3.0 and +2.3 kcal·mol^{-1} in solution. Although values in solution are somewhat closer to that estimated from experimental data, they predict an endothermic process. If one takes a closer look to the molecular geometries (Figure 2), it appears that the acidic proton is stabilized by hydrogen bonding in **2A** and **2A′**, whereas in **1A** is not. In **1A**, the proton is very exposed to the solvent molecules, explaining the large stabilization when the effect of the solvent is included in calculations. Comparison of IEF-PCM calculations with experimental value (+3.0 and +2.3 vs −1.7 kcal·mol^{-1}, respectively) shows that the continuum solvent models overestimate the stability of the reactants, i.e., the stabilization of the exposed acidic proton. Musaev and co-workers[28b] have also found the same energetic trend for the hydroperoxo formation on a divanadium-substituted anion. The authors reported that the reaction is exothermic in vacuum (−3.4 kcal·mol^{-1}), becoming slightly endothermic (+1.9 kcal·mol^{-1}) when the acetonitrile solvent effect is modeled. To further check the continuum solvation methodologies, we tested the new model recently developed by Truhlar and co-workers and implemented in Gaussian09 called SMD.[32] In this model, the bulk electrostatic contribution to free energy of solvation arises from IEF-PCM protocol using the SMD atomic Coulomb radii, whereas the bulk nonelectrostatic contribution follows the parametrization strategy of SM8 model.[33] The SMD method shows the same trend as IEF-PCM; the inclusion of the solvent disfavors the peroxo formation, but the computed value (−0.2 kcal·mol^{-1}) becomes quantitatively and qualitatively closer to the experimental one (−1.7 kcal·mol^{-1}).[34] Therefore, hereinafter we will use for discussion the more accurate continuum solvation model SMD. Nevertheless, we might consider vacuum and solvent energies as the lower and the upper energy limits of processes involving different stabilization of acidic protons.

Figure 3 shows the geometry for the transition state in the formation of the hydroperoxo intermediate (**TS1A**). The original titanium hydroxyl group captures an H atom from H_2O_2 to release a water molecule, and simultaneously a new bond between the Ti and the O atom of the OOH group is formed. The energy barrier computed in vacuum is quite low (8.2 kcal·mol^{-1}), and after including the solvent effects, it rises to 18 kcal·mol^{-1}. The increase in the energy barrier can be explained remembering the observed overstabilization of acidic protons by the continuum solvent model: there are 3 acidic protons exposed in the reactant, whereas in the transition state (**TS1A**) there are only two. Nevertheless, as we will show below, the higher value of the computed energy barrier is lower than the energy barrier of the next step of the catalytic cycle. Therefore, H_2O_2 activation is not the rate-limiting step, which agrees with the fast process observed.[10c]

The hydroperoxo (**2A**) POM may interconvert into the protonated peroxo (**2A′**) complex by proton transfer from the TiOOH moiety to the Ti−O−W bridging site. The calculated transition state (**TSA′** in Figure 3) leads to an energy barrier of 16.3 kcal·mol^{-1} in vacuum (16.2 kcal·mol^{-1} in solution). The value is not too high, suggesting that both species could interconvert under experimental conditions. Analogously, in situ XANES and EXAFS studies on TS-1 have shown the existence of equilibrium between side-on η^2 peroxo and end-on η^1 Ti-hydroperoxo groups.[35] Thus, from the analysis of the first step of the process (Scheme 1), we can conclude that the activation of hydrogen peroxide is not energetically demanding and yields the hydroperoxo complex, which then can interconvert with protonated peroxo complex overcoming a modest energy barrier.

Oxygen Transfer to Alkene in Ti-Monosubstituted Keggin Anions. Next, we turn our attention to the second step in the catalytic process, the oxygen transfer to alkene yielding the epoxide. Figure 4 collects the geometries of the transition states for oxygen transfer. In the case of titanium hydroperoxo species

(31) Cances, E.; Mennucci, B.; Tomasi, J. *J. Chem. Phys.* **1997**, *107*, 3032–3041.

(32) Marenich, A. V.; Cramer, C. J.; Truhlar, D. G. *J. Phys. Chem. B* **2009**, *113*, 6378.

(33) (a) Marenich, A. V.; Olson, R. M.; Kelly, C. P.; Cramer, C. J.; Truhlar, D. G. *J. Chem. Theory Comput.* **2007**, *3*, 2011. (b) Cramer, C. J.; Truhlar, D. G. *Acc. Chem. Res.* **2008**, *41*, 760. (c) Cramer, C. J.; Truhlar, D. G. *Acc. Chem. Res.* **2009**, *42*, 493.

(34) Additionally, we also re-computed the energy of the reactants (**1A** + H_2O_2) and the products (**2A** + H_2O) at the BP86 level using the conductor-like screening model (COSMO) as implemented in the ADF code to model acetonitrile effects. The COSMO method shows the same trend as the IEF-PCM method; the solvent disfavors the Ti hydroperoxo formation by about 7 kcal·mol^{-1} (8.8 kcal·mol^{-1} for IEF-PCM). For COSMO description, see: (a) Klamt, A.; Schüürmann, G. *J. Chem. Soc, Perkin Trans. 2* **1993**, 799.

(35) (a) Trubitsyna, T. A.; Kholdeeva, O. A. *Kinet. Catal.* **2008**, *49*, 371–378. (b) Bonino, F.; Damin, A.; Ricchiardi, G.; Ricci, M.; Spanó, G.; D'Aloisio, R.; Zecchina, A.; Lamberti, C.; Prestipino, C.; Bordiga, S. *J. Phys. Chem. B* **2004**, *108*, 3573–3583. (c) Prestipino, C.; Bonino, F.; Usseglio, S.; Damin, A.; Tasso, A.; Clerici, M. G.; Bordiga, S.; D'Acapito, F.; Zecchina, A.; Lamberti, C. *Chem. Phys. Chem.* **2004**, *5*, 1799–1804.

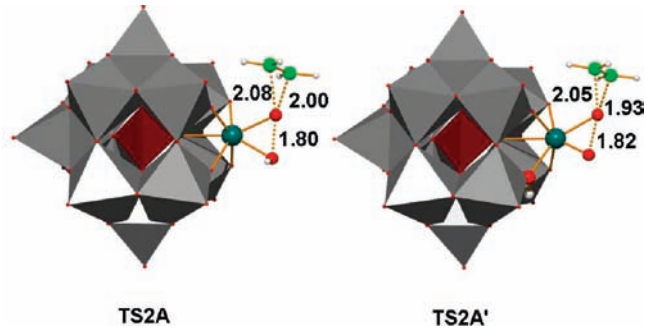

Figure 4. Transition state structures and main geometrical parameters for the oxygen transfer to the alkene from hydroperoxo (**TS2A**) and protonated peroxo species (**TS2A′**) in Ti-monosubstituted Keggin anion (distances in Å).

Scheme 2

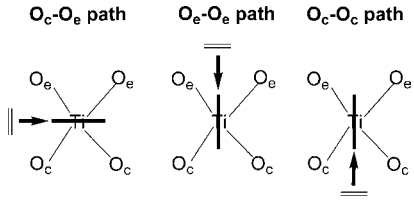

and following previous findings on theoretical studies,[19,23] we considerer that the alkene attacks to the proximal oxygen bound to titanium in a spiro orientation to the plane containing the Ti atom and the hydroperoxo oxygens (Figure 4). For titanium peroxo species both oxygen atoms are in principle equivalent. Both the hydroperoxo group in **2A** and the peroxo group in **2A′** are almost aligned with O−Ti−O plane forming an eclipsed conformation. However, at the corresponding transition states the O−O(H) and O−O moieties are rotated about 45° with respect to the eclipsed conformation and the alkene approaches to the hydroperoxo and peroxo groups bisecting the O−Ti−O angle. Thus, we first perform a systematic search of the possible approaches of the alkene substrate. The titanium center is bound to two different types of bridging Ti−O−W oxygens: O_c and O_e. The O_c oxygens link the TiW_2 triad with another triad (corner-sharing), whereas O_e are bridging oxygens inside the TiW_2 triad (edge-sharing). These oxygens can be used to define three different approaching paths of the alkene: O_c-O_c, O_e-O_e, and O_c-O_e (Scheme 2). Additionally, in the case of the peroxo species, it is possible to protonate either the corner-sharing or the edge-sharing oxygen, and then the alkene can approach through either the protonated side or the nonprotonated side. A more detailed description of the geometries and relative energies of the isomeric transition states is provided in Supporting Information. Interestingly, the lowest transition state for the hydroperoxo and peroxo paths are accessible from the previously computed **2A** and **2A′** structures.

Figure 4 shows the structures of the most stable transition states for oxygen transfer from hydroperoxo (**TS2A**) and protonated peroxo (**TS2A′**) species. Calculations reveal that the path starting from the Ti-hydroperoxo complex is the most favorable for oxygen transfer. The energy barriers are 24.3 and 27.3 kcal·mol^{-1} for hydroperoxo and peroxo paths, respectively, the transition state for hydroperoxo path being 1.7 kcal·mol^{-1} lower in energy than the peroxo one. After including the effect of the acetonitrile solvent the energy difference between the transition states rises from 1.7 to 5.4 kcal·mol^{-1}. Experimentally, the epoxidation of alkenes is observed only by increasing proton amount in the monotitanium-substituted POM. Thus, the nonprotonated peroxo anion $[PTi(O_2)W_{11}O_{39}]^{5-}$ is inactive toward the oxidation of alkenes and other organic substrates,[36] whereas the protonated titanium POMs $[Na_{5-n}H_nPTi(O_2)W_{11}O_{39}]$ ($n = 1-5$) become active, favoring the heterolytic mechanism (epoxide and diol products) as the number of protons increase.[37] In light of the experimental data and our theoretical results, it is reasonable to think that increasing the proton amount would facilitate the protonation at the peroxo ligand, forming the less stable but more reactive η^1-hydroperoxo intermediate.

Table 1. Geometrical Parameters, Natural Population, and Natural Bond Orbital Analysis for $[PTi(OOH)W_{11}O_{39}]^{4-}$ (**2A**) and $[HPTi(O_2)W_{11}O_{39}]^{4-}$ (**2A′**) Anions[a]

	$[PTi(OOH)W_{11}O_{39}]^{4-}$ (**2A**)	$[HPTi(O_2)W_{11}O_{39}]^{4-}$ (**2A′**)
d (O−O)	1.44	1.45
σ^*_{O-O} (energy)	+11.3 eV	+11.2 eV
σ^*_{O-O} (population)	0.01	0.05
q_{NPA} (O_α)	−0.40	−0.39
q_{NPA} (O_β)	−0.46	−0.38
Δq_{NPA} ($O_\alpha-O_\beta$)	0.06	0.01
q_{NPA} (Ti)	1.48	1.47

[a] Energies in kcal·mol^{-1}, distances in Å, and atomic charges and populations in au.

To understand the origin of the higher reactivity of hydroperoxo species with respect to the peroxo one, we have analyzed in more detail the electronic structures of both intermediates by means of natural bond orbital (NBO) analysis.[38] Table 1 summarizes the results. According to previous reports on alkene epoxidation by Ti-containing catalysts, the oxygen transfer proceeds through a nucleophilic attack of the alkene, in which the $\pi_{C=C}$ orbital of the alkene transfer electrons to the σ^*_{O-O} orbital of the Ti-OO(H) group.[23] Here the nucleophilic character of the alkene attack is also manifested through the NPA electron density transfer in the transition states **TS2A** and **TS2A′**, about 0.3 e, from the alkene to the peroxo and hydroperoxo anions. Within this model, the lower the energy of the σ^*_{O-O} orbital, the smaller the activation barrier for oxygen barrier because it favors the interaction with the $\pi_{C=C}$ orbital of the alkene. However, we do not observe this trend when comparing the two different functional groups. The calculated energy of the σ^*_{O-O} NBO orbital is slightly higher for the more reactive hydroperoxo species **2A** (+11.3 eV) than for less reactive peroxo species **2A′** (+11.2 eV). Alternatively, the polarization of the O−O bond in the intermediate could be an important factor determining the differences in the activity.[24a] In the case of hydroperoxo species, the σ^*_{O-O} orbital is polarized toward the proximal O_α oxygen, which helps the donor−acceptor interactions with the double bond. As a result of O−O bond polarization, the distal O_β oxygen gains some negative charge, and in turns the proximal O_α oxygen becomes more positively charged (see values in Table 1). The decrease in the charge of the attacked proximal O_α oxygen is expected to increase the electrophilicity of the hydroperoxo ligand and its activity toward oxygen transfer to a nucleophile. Simultaneously, the negative

(36) Yamase, T.; Ishikawa, E.; Asai, Y.; Kanai, S. *J. Mol. Catal. A: Chem.* **1996**, *114*, 237–245.
(37) Kholdeeva, O. A.; Trubitsina, T. A.; Timofeeva, M. N.; Maksimov, G. M.; Maksimovskaya, R. I.; Rogov, V. A. *J. Mol. Catal. A: Chem.* **2005**, *232*, 173–178.
(38) Glendening, E. D., Reed, A. E. Carpenter, J. E.; Weinhold, F. *NBO version 3.1, Gaussian03*; Gaussian, Inc.: Wallingford, CT, 2004.

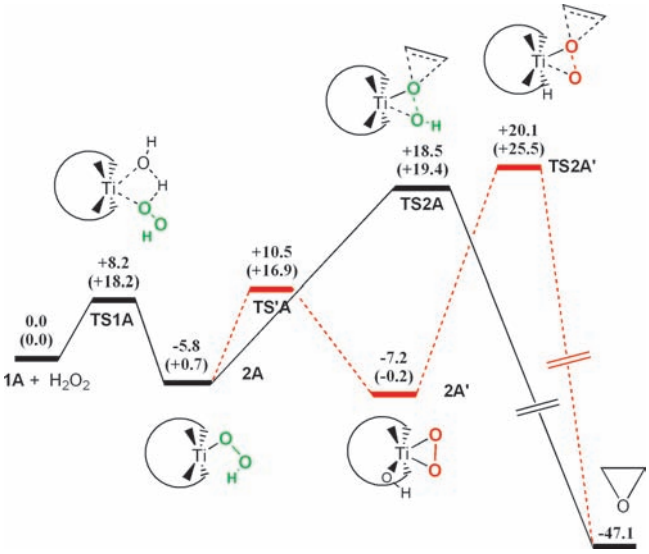

Figure 5. Calculated potential energy profile (kcal·mol^{-1}) for the ethene epoxidation with H_2O_2 by $[PTi(OH)W_{11}O_{39}]^{4-}$ (**1A**) in vacuum. Values in parentheses correspond to SMD calculations. Dashed lines correspond to the less favorable peroxo path.

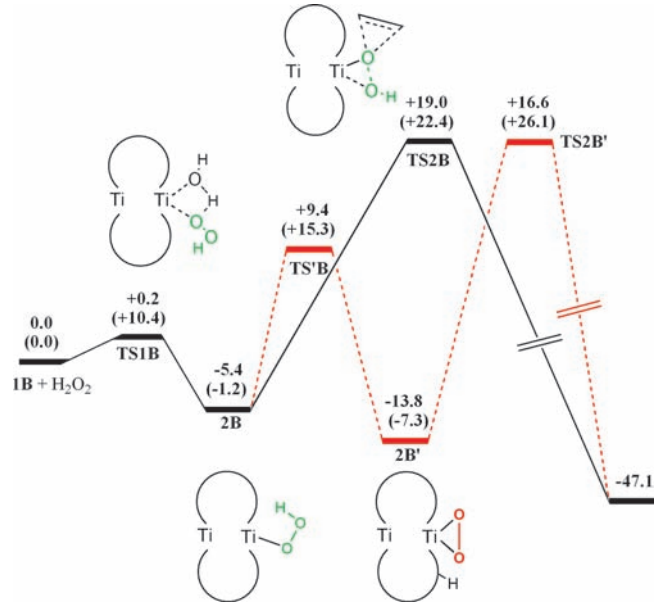

Figure 6. Calculated potential energy profile (kcal·mol^{-1}) for the ethene epoxidation with H_2O_2 by $[Ti_2(OH)_2As_2W_{19}O_{67}]^{8-}$ (**1B**) in vacuum. Values in parentheses correspond to SMD calculations. Dashed lines correspond to the less favorable peroxo path.

charge at the O_β oxygen would be stabilized by the interaction with the positively charged titanium center via donation from the filled p orbital of O_β oxygen to empty d orbitals of Ti. These reasonings agree well with the lower computed energy barriers for hydroperoxo species. Thus, the proton in the hydroperoxo group polarizes the O−O bond and favors its heterolytic cleavage ($\Delta q(O_\alpha - O_\beta) = 0.06$ e in **2A** vs 0.01 e in **2A′**). In agreement with previous explanation, when we include the effect of a polar solvent such as acetonitrile the energy difference between the transition states rises from 1.7 to 5.4 kcal·mol^{-1} due to a larger stabilization of the more polar hydroperoxo transition state in **TS2A**.

Figure 5 collects the overall energy profile of the epoxidation process. To summarize, the overall proposed mechanism can be divided in two steps. In the first step, the hydrogen peroxide approaches to the titanium hydroxo POM and transfers the hydrogen atom to the Ti-OH group, forming a titanium hydroperoxo (Ti-OOH) and loosing a water molecule in a concerted manner. The process is slightly exothermic with an energy barrier below 18 kcal·mol^{-1}. Additionally, a titanium peroxo species can be formed from the titanium hydroperoxo species via proton transfer to a bridging Ti−O−W oxygen. The energy barrier is not too high, about 16 kcal·mol^{-1}, and the energy difference between both species is not too large, about 1 kcal·mol^{-1} in favor of peroxo complex. Thus, presumably both species coexist under experimental conditions. The second step consists of an oxygen transfer to the alkene to form the epoxide. Although the hydroperxo species is less stable than the peroxo one, the hydroperoxo is more reactive with an energy barrier in vacuum of 24.3 kcal·mol^{-1} (25.7 kcal·mol^{-1} by the case of a rapid pre-equilibrium between hydroperoxo and peroxo species). The solvent effects reduce the energy barrier in about 5 kcal·mol^{-1}, which is probably an overestimated amount (see discussion above). Nevertheless, we can estimate an energy barrier of over 20 kcal·mol^{-1}, concluding that oxygen transfer process is the rate-limiting step of the entire catalytic cycle.

Dititanium-Substituted POM Anions: Effect of the Coordination Environment. As described in more detail in the introduction, the sandwich-type dititanium 19-tungstodiarsenate(III) (**1b**) is active in alkene oxidation with H_2O_2 and leads selectively to products typical of a heterolytic oxidation mechanism. Dititanium complex **1b** possesses an *unusual* 5-coordinated titanium environment, which contrasts with the 6-coordinated titanium atom in the Keggin anion **1a**. We use the differences between these soluble probes with well-defined Ti environments to gauge the effect of coordination on the Ti-containing catalysts. Figures 6 and 7 show the computed energy profiles and the most important structures. In overall, the results for **1A** and **1B** are qualitatively similar; however, some differences between 6-coordinated Ti (**A**) and 5-coordinated (**B**) environments merit a more detailed discussion. First, in vacuum the stabilization energy of the peroxo complex is somewhat larger for the 5-coordinated titanium (ΔE(**2B** → **2B′**) = −8.4 kcal·mol^{-1}) than for the 6-coordinated one (ΔE(**2A** → **2A′**) = −1.4 kcal·mol^{-1}). Upon formation of the η^2 side-on peroxo species, the titanium center increases its coordination, becoming heptacoordinated for the Keggin structure (**2A′**). Second, the hydrogen peroxide activation by 5-coordinated titanium center (**TS1B**) requires a lower amount of energy (about 8 kcal·mol^{-1}) than activation by 6-coordinated titanium (**TS1A**). Similar to the Ti-Keggin POM, the energy barrier for oxygen transfer from hydroperoxo complex **2B** is lower than that from peroxo one **2B′**: +24.4 vs +30.4 kcal·mol^{-1} in vacuum and +23.6 vs +33.4 kcal·mol^{-1} in solution. In the sandwich Ti-POM, the oxygen transfer process is also the rate-limiting step of the entire catalytic cycle.

To analyze in more detail the effect of the titanium environment on the catalytic performance, we confront the computed values with experimental results. Making use of transition state theory, one can estimate the overall activation barrier of the catalytic process from turnover frequency (TOF) values, assuming that they can be assimilated to an overall rate constant.

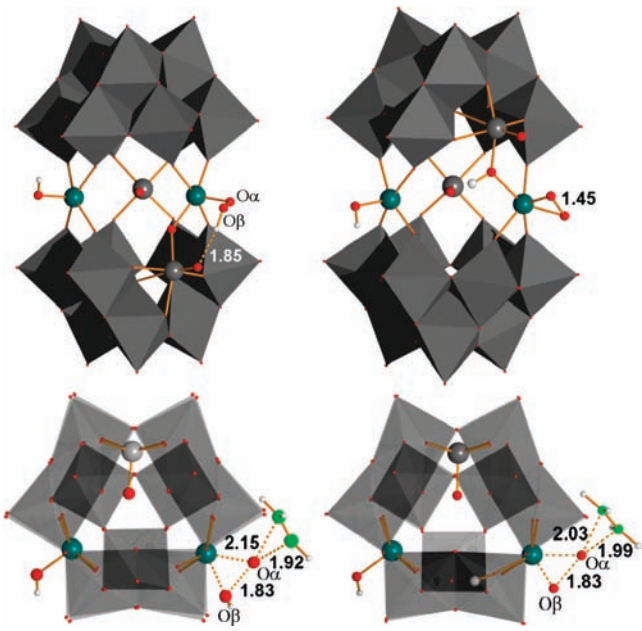

Figure 7. Optimized structures for hydroperoxo intermediate **2B**, protonated peroxo intermediate **2B′**, and transition states **TS2B** and **TS2B′** (distances in Å).

The TOF for cyclohexene epoxidation catalyzed by Ti-disubstituted POM $[Bu_4N]_8[Ti_2(OH)_2As_2W_{19}O_{67}(H_2O)]$ in acetonitrile is 11.3 h^{-1} with 100% substrate conversion,[12a] which leads to an estimated overall activation barrier of 24.1 kcal·mol^{-1}. Our computed energy barrier for the oxygen transfer process through the hydroperoxo path in vacuum is 24.4 kcal·mol^{-1}, which fits quiet well with the experimental value. The catalytic activity of $[Bu_4N]_8[Ti_2(OH)_2As_2W_{19}O_{67}(H_2O)]$ was higher than for the dimer $[Bu_4N]_7[(PTiW_{11}O_{39})_2OH]$ (TOF = 2.1 h^{-1} and 45% conversion at the same experimental conditions).[12a,39] In this case, where the titanium center is 6-fold coordinated, the TOF leads to an estimated overall activation barrier only slightly higher, 25.3 kcal·mol^{-1}. From the kinetic data obtained for the Ti-monosubstituted Keggin POMs $Na_{5-n}H_nPTiW_{11}O_{40}$ with $n = 2-5$,[37] we estimated energy barriers ranging from 24.9 to 25.1 kcal·mol^{-1}, indicating intermediate activities between the dimer and dititanium POMs. Thus, the observed activity differences are translated in small energy differences of activation barriers (about 1 kcal·mol^{-1}), and consequently subtle effects are expected to be responsible for them. In agreement with the small differences, the computed energy barrier for the hydroperoxo path in the Ti-monosubstituted Keggin (24.3 kcal·mol^{-1}) is very close to that in the dititanium POM (24.4 kcal·mol^{-1}). If we regard the Ti-OOH moiety of hydroperoxo intermediates **2A** and **2B**, we observe very similar geometrical and electronic parameters. The O−O bond distances are 1.44 Å for both intermediates, and the O−O bond polarization is almost equal ($\Delta q(O_\alpha - O_\beta) = 0.06$ and 0.05 e in **2A** and **2B**, respectively). Thus, the 5-coordinated titanium environment in **1** can tune the activity of the hydroperoxo species but does not have a dramatic influence.

(39) For the parent non-protonated dimer $[Bu_4N]_8[(PTiW_{11}O_{39})_2O]$ a similar TOF (3.4 h^{-1}) was determined for cyclohexene oxidation, indicating a similar activity for both dimers. The TOF was obtained at values of temperature (50 °C) and substrate concentration (CyH = 0.2 M, H_2O_2 = 0.2 M) that are only slightly different than those for $[Bu_4N]_7[(PTiW_{11}O_{39})_2OH]$.[37] Details on the new experimental data will be published elsewhere.

It is also interesting to compare our results with other theoretical studies on molecular models covering different Ti coordination environments. The computed oxygen transfer barrier from Keggin hydroperoxo complex **2A** (+24.3 kcal·mol^{-1}) is very similar to that reported for the analogous 6-coordinated titanium cluster $Ti(OH)_3(H_2O)_2(\eta^1\text{-OOH})$, +24.4 kcal·mol^{-1}.[23] On the other hand, the barrier from dititanium hydroperoxo complex **2B** (24.4 kcal·mol^{-1}) is considerably higher than those for cluster models with five ligands such as the T6 model of TS-1 catalysts (+9 kcal·mol^{-1})[24] and the $Ti(OH)_3(H_2O)(\eta^2\text{-OOH})$ complex (+13 kcal·mol^{-1}).[23] Other even lower coordinated clusters of the type $Ti(OR)_3(\eta^2\text{-OOH})$ (R = SiH_3,[20b] CH_3,[19] H[23]) show also lower barriers ranging from 10 to 15 kcal·mol^{-1}. We can deduce a plausible explanation for the differences in energy barriers for hydroperoxo species from the observations of Root and co-workers.[24] These authors conclude that the flexibility of Ti centers to accommodate 6-fold octahedral coordination is crucial to stabilize the transition state. In the Keggin-type POM, the transition state (**TS1A**) becomes 7-fold coordinated because the simultaneous Ti−O bond-breaking/bond-making (see Figure 4). Hence, the Ti environment exceeds the optimal 6-fold coordination and raises the energy barrier. In dititanium-type POM, the transition state (**TS1B**) is 6-fold coordinated but is not flexible enough to adopt an octahedral structure. In agreement with this, the η^2-coordination of the OOH group is only observed when the Ti center adopts 6-fold octahedral rearrangement or has a lower coordination number. The latter requirement is not fulfilled by dititanium POMs **2B**, which exhibit a rigid square planar Ti(O-W)$_4$.

Origin of the Epoxidation Activity. We have also examined other possible factors explaining the differences in catalytic performance for the sandwich-type dititanium anion. We consider the possibility of a cooperative effect between the two titanium centers via formation of an intramolecular hydrogen bonding. Berkessel and co-workers have proposed that the peroxo titanium intermediate can be activated by intramolecular hydrogen bonding in titanium-salalen catalysts.[40] To check the reliability of an intramolecular interaction involving the TiOOH moiety, we have computed a dihydroperoxo intermediate $[Ti_2(OOH)_2As_2W_{19}O_{67}]^{8-}$, in which the two TiOOH functional groups are placed in their mutually closest conformation. However, the relative orientation of the two titanium centers in sandwich-type POM does not allow for intramolecular hydrogen bonding formation, the O_β-H···O_β(H) distance being 7.44 Å (see Figure S3 in Supporting Information).

The group 4 metal-substituted Keggin POMs exhibit a strong tendency for intermolecular linkage formation resulting in dimeric structures.[10a,41] In fact, previous experimental studies showed that partial dimerization of the titanium-monosubstituted Keggin POMs accompanies the reaction to yield the titanium peroxo species.[10c] On the other hand, in dititanium-substituted sandwich-type POM, dimerization is not likely because of steric shielding caused by the tungsten groups adjacent to the titanium centers.[12a] Thus, dimerization could play a role in the differences in catalytic performance. To check this hypothesis, we built a new energy profile for Ti-monosubstituted Keggin POMs combining data from calculations and from experimentally

(40) Berkessel, A.; Brandenburg, M.; Leitterstorf, E.; Frey, J.; Lex, J.; Schäfer, M. *Adv. Synth. Catal.* **2007**, *349*, 2385–2391.
(41) Kholdeeva, O. A.; Maksimov, G. M.; Maksimovskaya, R. I.; Vanina, M. P.; Trubitsina, T. A.; Naumov, D. Y.; Kolesov, B. A.; Antonova, N. S.; Carbó, J. J.; Poblet, J. M. *Inorg. Chem.* **2006**, *45*, 7224–7234.

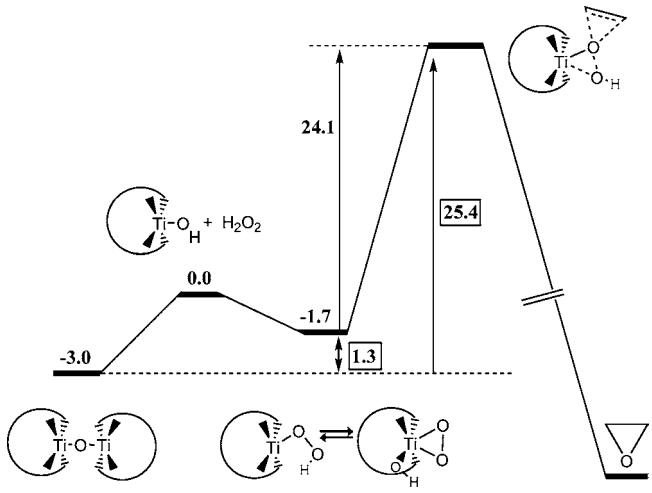

Figure 8. Potential energy profile (kcal·mol^{-1}) for the ethene epoxidation with H_2O_2 by monosubstituted Keggin anion derived from experimental data.

determined equilibrium constants (Figure 8). The equilibrium constant (K_1 =10) for the reaction of hydroxo $[Bu_4N]_4[PTi(OH)W_{11}O_{39}]$ complex (**1a**) with H_2O_2 to give the peroxo complex and water led to a relative energy for the products of −1.7 kcal·mol^{-1}, and the equilibrium constant (K_2 = 0.006) for the hydrolysis of μ-oxo dimer $[Bu_4N]_8[(PTi\ W_{11}O_{39})_2O]$ to yield **1a** leads to a relative energy for the dimer of −3.0 kcal·mol^{-1}. Consequently, Keggin dimer should be around 1.3 kcal·mol^{-1} more stable than the corresponding protonoted peroxo monomer. This causes a shift on the rate-determining intermediate (the lowest energy species involved in the catalytic cycle), which becomes the dimer. In this case, the overall process governing the activity would go from the dimer to the oxygen transfer. If we assume computational findings, which show that the energy barrier for oxygen transfer in the Ti Keggin POM is the same as in the dititanium sandwich POM, the overall energy barrier should raise around 1 kcal·mol^{-1} for Ti Keggin species as a result of the formation of lower energy dimeric species (see Figure 8). This latter value nicely fits with the differences estimated from the experimental TOF values; the estimated barrier for dimer $[Bu_4N]_7[(PTiW_{11}O_{39})_2O]$ complex[39] is about 25 kcal·mol^{-1} and for the sandwich $[Bu_4N]_8[Ti_2(OH)_2As_2W_{19}O_{67}(H_2O)]$ catalysts about 24 kcal·mol^{-1}. Therefore, we can conclude that the formation of dimeric species would slow down the reaction.

Very recently, Kessler and co-workers have questioned the extended view of the influence of titanium coordination on both the activity and the selectivity of the epoxidation process, by analyzing the experimentally determined outcome of silica-grafted titanium oxide models such as titanosilsesquioxanes. The authors suggest that for these compounds the secret to achieve efficiency probably lies in avoiding the formation of large particles of titanium, where the metal atoms are not easily accessible for the coordination and release of peroxide ligands.[42] It interesting to note the similarity between the suggestions of Kessler and co-workers and the discussion derived from our results. For titanium-substituted POMs, the formation of higher aggregates of titanium, such as dimers, causes a loss in the efficiency of the catalysts. In this line, Kholdeeva et al. found

Scheme 3

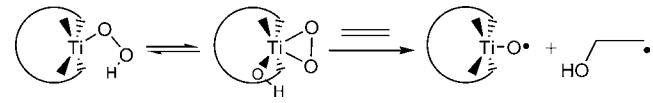

that the rate of thioether oxidation with H_2O_2 catalyzed by Ti-substituted Keggin anions increased with increasing H_2O concentration, showing that this is caused by the dissociation of the dimer to the monomer.[10d] With all of the results in hand, we believe that it is possible to define several requirements for the design of more active Ti-containing catalysts: (i) 5-fold (or lower) Ti coordination environments, (ii) flexible Ti centers, and (iii) easily reagent-accessible Ti sites.

Origin of Selectivity toward Heterolytic Products. Not all Ti-based catalysts are effective in alkene epoxidation because of the contribution of a radical mechanism yielding homolytic oxidation products. This latter group includes the monoprotonated Ti(IV)-substituted Keggin-type POMs and Zr(IV)-substituted Keggin-type POMs.[41] The one-electron oxidation mechanism of the alkenes would involve a homolytic cleavage of the O−O bond and would lead to the formation of a M^{IV}-O$^{\bullet}$ species and an oxyalkyl (or hydroxyalkyl) radical intermediate, which later deprotonates to yield ene-one (or ene-ol) products. It is out of the scope of this work to study in detail the homolytic mechanism, but it would be interesting to gauge the feasibility of forming radical intermediates as a function of the metal nature and its environment. To do that, we computed the energy of the formation of metallaoxyl and hydroxyethyl radicals from the corresponding protonated peroxo anions (Scheme 3) for Ti- and Zr-monosubstitued Keggin-type POMs and Ti-disubstituted POM. The selected process does not involve charge separation to avoid the difficulties of accurate accounting of solvent effects for differently charged species. We did not observe reduction of the metal center to TM(III) for any of the substituted POMs, the calculated spin densities at the terminal oxygen atoms ranging from 0.91 to 0.98 e. The energy estimates for the formation of radical intermediates from Ti- and Zr-monosubstituted Keggin POMs are 25 and 26 kcal·mol^{-1}, respectively. These values are lower than that for the Ti sandwich POM (31 kcal·mol^{-1}), suggesting that the homolytic O−O bond cleavage in the latter complex is energetically disfavored, which agrees with the observed increased selectivity for Ti sandwich POM **1a** and also with lower rates of H_2O_2 decomposition in the absence of alkene.[12b]

Effect of the Metal Nature on the Oxygen Transfer Mechanism. Apart from Ti(IV), many other catalytic systems containing high-valent d^0 early transition metal such as V(V), Mo(VI), W(VI), and Re(VII) have been reported to be effective for the epoxidation of alkenes with H_2O_2.[43] Among them we also found polyoxometalate-based catalysts such as the divanadium-substituted polyoxometalate $[\gamma\text{-}1,2\text{-}H_2SiV_2W_{10}O_{40}]^{4-}$ (γ-V_2-POM)[44] and the lacunary polyoxometalate $[\gamma\text{-}H_4SiW_{10}O_{36}]^{4-}$ (γ-W_{10}-POM).[45] DFT calculations proposed that the oxygen transfer occur from a hydroperoxo intermediate for γ-W_{10}-POM,[28a] whereas for γ-V_2-POM the peroxo-type mechanism is predicted.[28b,29a] In a review of theoretical studies on mono-

(42) Viotti, O.; Seisenbaeva, G. A.; Kessler, V. G. *Inorg. Chem.* **2009**, *48*, 9063–9065.

(43) For recent review, see: (a) Grigoropoulou, G.; Clark, J. H.; Elings, J. A. *Green Chem.* **2003**, *5*, 1–7.

(44) Nakagawa, Y.; Kamata, K.; Kotani, M.; Yamaguchi, K.; Mizuno, N. *Angew. Chem., Int. Ed.* **2005**, *44*, 5136–5141.

(45) Kamata, K.; Yonehara, K.; Sumida, Y.; Yamaguchi, K.; Hikichi, S.; Mizuno, N. *Science* **2003**, *300*, 964–966.

Table 2. Oxygen Transfer Energy Barriers and Natural Bond Orbital Analysis for Peroxo $[HPTM(O_2)W_{11}O_{39}]^{n-}$ and Hydroperoxo $[PTM(OOH)W_{11}O_{39}]^{n-}$ Anions[a]

	peroxo $[HPTM(O_2)W_{11}O_{39}]^{n-}$				hydroperoxo $[PTM(OOH)W_{11}O_{39}]^{n-}$			
TM	$\Delta E^{\ddagger}$	$q_{(O\alpha)}$	σ^*_{O-O}	d_{TM-O}	$\Delta E^{\ddagger}$	σ^*_{O-O}	d_{TM-O}	σ_{TM-O} (% TM)
Ti(IV)	+27.3	−0.38	+2.1	1.84	+24.3	+2.4	1.84	14
V(V)	+23.9	−0.19	+1.8	1.81	+30.6	+2.1	1.78	20
Zr(IV)	+25.7	−0.58	+1.8	2.01	+12.1	+2.3	2.02	9
Nb(V)	+19.9	−0.40	+1.0	1.94	+14.0	+1.6	1.94	14
Mo(VI)	+12.3	−0.27	+0.4	1.91	+16.8	+1.3	1.89	19
W(VI)	+12.0	−0.35	−0.1	1.90	+15.0	+1.0	1.88	17
Re(VII)	+1.3	−0.23	−0.8	1.87	+16.5	+0.2	1.87	23

[a] Energies in kcal·mol^{-1}, distances in Å, and atomic charges and populations in au.

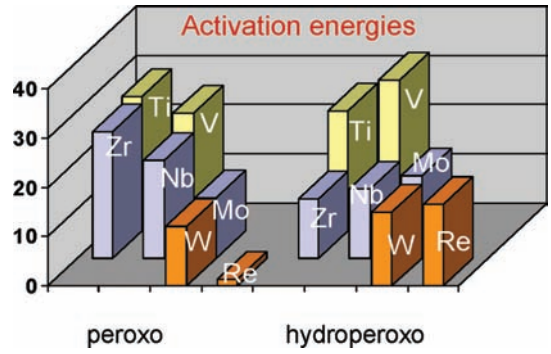

Figure 9. Activation energies (in kcal·mol^{-1}) associated with the oxygen transfer (step 2 in Scheme 1) computed for $PTMW_{11}$ Keggin anions in vacuum.

metallic complexes,[46] Deubel et al. have discussed that protonation of a peroxo ligand (formation of hydroperoxo functionality) may result in an activation of the catalysts toward alkene epoxidation. The authors concluded that the *hydroperoxo* mechanisms are less important in Re(VII), competitive in Mo(VI), and more relevant in Ti(IV) catalysts. More recently, Pecoraro, Gioia, and co-workers have also proposed by means of DFT calculations that protonation plays a role in the activation of peroxo form of V(V) haloperoxidase.[47] To better understand the effect of the metal and the role of protonation on the peroxo functionality, it is worth comparing the titanium-substituted POMs with other early transition metal based complexes. To allow a straightforward comparison and in order to asses the effect of the metal within an inorganic oxide matrix, we performed a systematic study on fully oxidized early transition metal substituted Keggin POMs $[PTM(O_2)(H)W_{11}O_{39}]^{n-}$ (TM = Ti(IV), V(V), Zr(IV), Nb(V), Mo(VI), W(VI), and Re(VII)).

Table 2 collects the calculated energy barriers in vacuum for the oxygen transfer process to ethene from peroxo and hydroperoxo species (step 2 in Scheme 1), as well as some selected parameters from electronic population (NBO)[48] and structural analysis. The first striking feature observed is that energy barriers for peroxo and hydroperoxo mechanisms follow *opposite* trends. When we move from the left to the right in the periodic table, the energy barrier for the peroxo path lowers significantly, while the energy barrier for hydroperoxo path rises slightly as shown in the graphical representation given in Figure 9. Going down from the first to the second TM row, both peroxo and hydroperoxo energy barriers decrease, but the latter do it significantly. Overall, several conclusions emerge from the energy values in Figure 9: (1) the peroxo mechanism is disfavored in Ti Keggin anions and in related structures, the hydroperoxo path being the most plausible, (2) the peroxo mechanism is more favorable in TMs in high oxidation states, and (3) TM atoms with a high oxidation state would be more adequate for epoxidation reactions if we consider only the oxygen transfer step.

Concerning the last conclusion, the reader should take into account that H_2O_2 activation (step 1 in Scheme 1) is also very sensitive to the nature of the metal. An extensive discussion about this point will be developed in future works, but here we wish to comment briefly the case of TM = W. It was shown previously that metals with lower oxidation states, such as Ti(IV), increase the nucleophilicity of the substituted region of the POM facilitating the protonation,[11] and consequently, the formation of the reactive terminal hydroxyl ligands. On the other hand, the W(VI) atoms form stronger W=O bonds and less basic sites. Here, the protonation occurs preferably at the bridging W−O−W oxygens,[11] preventing the activation of W=O groups to react with H_2O_2. Accordantly, the computed energy barrier in vacuum for H_2O_2 activation by $[PW(OH)W_{11}O_{39}]^{2-}$ (16.5 kcal·mol^{-1}) is 2-fold larger than for **1A** (8.2 kcal·mol^{-1}), and adding the protonation energy of the W=O group from the most stable W−O(H)−W species, the barrier rises above 30 kcal·mol^{-1}. This would explain why, for example, the sandwich tungstate $TBA_6[As_2W_{21}O_{67}(H_2O)]$ is not active in alkene epoxidation,[12] whereas the lacunary POM $[\gamma\text{-}H_4SiW_{10}O_{36}]^{4-}$ with four terminal hydroxyl ligands is active and selective.[28a,45]

Finally, we will discuss why peroxo and hydroperoxo mechanism follow different trends for different TM atoms. With increasing positive charge of the metal, we expect a higher eletrophilicity of the corresponding TM-OO peroxo unit. This is manifested in less negative atomic charges supported by the peroxo oxygens and in a lower energy of the σ^*_{O-O} orbitals in peroxo anions (Table 2). Thus, in agreement with reactivity models previously reported,[46] the more electrophilic the inorganic peroxide, the lower is the energy barrier for oxygen transfer from peroxo species. Surprisingly, the energy barriers for hydroperoxo species do not follow the latter trend. To check whether there is a change in the reactivity model, the electron density transfer at the hydroperoxo transition states is analyzed. For all substituted POMs, the NPA analysis indicates that the transfer occurs from the alkene to the hydroperoxo complex (values ranging from +0.28 to +0.37 e), manifesting the electrophilic nature of the hydroperoxo ligand. Thus, for the considered series of hydroperoxo species, the contribution of the σ^*_{O-O} energy level to the activation energy should be considered a second order effect. Alternatively, within a row we observe a correlation between the TM-O_α bond length and the hydroperoxo activation barrier: the shorter the bond, the larger the barrier. We analyze in more detail the TM-O_α bonds with the help of NBO charge analysis. For the second row, the contributions of d-Zr, -Nb, and -Mo orbitals to the TM-O_α bond are 9%, 14%, and 19% for σ interaction and 10%, 16%, and 22% for π interaction. The increased metal contributions on going from the left to the right in the periodic table are due to the lowering of the empty d-type orbitals of the metal, which

(46) Deubel, D. V.; Frenking, G.; Gisdakis, P.; Herrmann, W. A.; Rösch, N.; Sundemeyer, *J. Acc. Chem. Res.* **2004**, *37*, 645–652.
(47) Zampella, G.; Fantucci, P.; Pecoraro, V. L.; De Gioia, L *J. Am. Chem. Soc.* **2005**, *127*, 953–960.
(48) The orbital energies and compositions were calculated including solvent effects in order to allow direct comparison of differently charged species.

favors their mixing with the filled oxygen p orbitals. This causes a strengthening of the TM-O_α bond and a decreasing of calculated bond distances. Thus, the direct contribution of TM-O bond strength to the activation barrier seems to play a key role, while the electrophilicity of the O−O moiety tunes the reactivity. The combination of both effects results in increased energy barriers on going up and right in the periodic table. In the case of Ti-substituted POMs, the relatively low electrophilicity would be compensated by a weaker Ti−O bonding.

Upon protonation of the peroxo unit, in principle one should expect a lowering of the σ^*_{O-O} energy level and of the electrophilicity due to the electrostatic field generated by the additional proton. However, in the considered cases, protonation is accompanied by a shift in coordination mode from η^2-O_2 to η^1-OOH, disfavoring the overlap between the σ^*_{O-O} orbital and the d-type orbitals of the substituted metal. The latter effect counterbalances the electrostatic one, and as a result, the calculated energies of σ^*_{O-O} orbital for η^1-OOH hydroperoxo species are, in general, slightly higher than for η^2-O_2 peroxo ones. Note also that, as discussed above, the energy barriers for the peroxo and hydroperoxo paths follow different trends along the periodic table.

Conclusions

An extensive DFT study has been carried out to understand the reaction mechanisms of alkene epoxidation catalyzed by Ti- and other TM-substituted polyoxometalates. The reaction proceeds in two steps, the activation of hydrogen peroxide and the oxygen transfer to the alkene from the hydroperoxo Ti-OOH intermediate, the latter being the rate-limiting step. The protonated peroxo intermediate TiOO is thermodynamically slightly more stable, but the polarization of the O−O bond in the hydroperoxo species is responsible for the higher reactivity of this species. On going from the 6-coordinated Ti environment in monosubstituted Keggin-type anion (**1A**) to the 5-coordinated in dititanium sandwich anion (**1B**), the energy profile changes only slightly. However, the steric shielding of tungsten groups adjacent to Ti centers prevents the formation of higher aggregates in dititanium sandwich anion, which improves the efficiency of the catalysts. By comparison with previous calculations on cluster models, we also suggest that the design of Ti centers with lower coordination and/or more flexibility would also improve catalytic performance. The higher selectivity observed for the dititanium sandwich anion is likely related to the higher energy associated with the homolytic O−O bond breaking in the hydroperoxo intermediate for the dititanium polyoxometalate.

When we move from the left to the right and down in the periodic table, the formation of the epoxide via peroxo intermediate becomes competitive because of the higher mixing between the orbitals of the TM and the O−O unit, which is less effective in the hydroperoxo mechanism. For TM = W(VI) the oxygen transfer occurs via the oxo mechanism with a relatively low energy barrier, but the limiting step is the activation of H_2O_2.

Experimental Section

Computational Details. Calculations were performed with the Gaussian03 package[49] and NBO program (version 3.0)[38] at the DFT level by means of the hybrid exchange-correlation B3LYP[50] functional. For Ti, W, and As atoms, the LANL2DZ pseudopotential was used.[51] The 6-31G(d, p) basis set[52] was used for the C and H atoms, as well as for the O atoms of hydrogen peroxide and directly bound to Ti. For the remaining atoms, we employed a 6-31G basis set.[52] Geometry optimizations in gas phase of all reactants, intermediates, and transition states were performed without any symmetry constrains. Solvent effects were included by means of SMD model[32] single point calculations as implemented in Gaussian09,[53] using the most common experimental reported acetonitrile (dielectric constant, $\varepsilon = 36.64$). Initially, the IEF-PCM[32] solvent model was considered, but during revision of the manuscript the SMD model[32] was revealed to be more accurate for the systems under study (see text for details). For Keggin-type anions, transition states were characterized by a single imaginary frequency and the normal mode, which corresponds to the expected reaction path. For dititanium sandwich-type anions with an increased number of atoms and basis set functions, it was not possible to compute the Hessian matrix with our current computational resources. To ensure the transition state nature, a particular computational protocol was defined. First we performed a partial geometry optimization, freezing the reactive center at the geometry of the corresponding Keggin-type transition state (TS). Then, we computed the Hessian with a smaller basis set (BS2) and checked that the largest imaginary frequency corresponded to the searched reaction path. Finally, we used Hessian calculated with BS2 to search the TS with the larger basis set. In the basis set BS2, for the atoms involved in the reaction center (Ti, C, H, and O of H_2O_2 and directly bound to Ti), the same type of basis sets were used, whereas for the rest of the O atoms the sto-3g[54] basis set was used, and for W and As atoms the LANL2MB pseudopotential[51] was used. The natural bond orbital (NBO) method[38,55] was used to compute atomic charges and to analyze the resultant wave function in terms of optimally chosen localized orbitals, localized orbitals corresponding to a Lewis structure representation of chemical bonding.

Acknowledgment. This work was supported by the Spanish MICINN [CTQ2008-06549-C02-01/BQU and by the Generalitat de Catalunya (2009SGR-00462 and XRQTC). N.S.A. thanks the MICINN for a predoctoral fellowship. O.A.K. thanks the Russian Foundation for Basic Research (grant- 09-03-91333).

Supporting Information Available: Tables containing *xyz* coordinates for most relevant structures reported in this paper and complete refs 49 and 53. This material is available free of charge via the Internet at http://pubs.acs.org.

JA1023157

(49) Frisch, M. J.; et al. *Gaussian 03*, revision B.03; Gaussian, Inc.: Pittsburgh, PA, 2004.
(50) (a) Lee, C.; Yang, C.; Parr, R. G. *Phys. Rev. B* **1988**, *37*, 785–789. (b) Becke, A. D. *J. Chem. Phys.* **1993**, *98*, 5648–5652. (c) Stephens, P. J.; Devlin, F. J.; Chabalowski, C. F.; Frisch, M. J. *J. Phys. Chem.* **1994**, *98*, 11623–11627.
(51) Hay, P. J.; Wadt, W. R. *J. Chem. Phys.* **1985**, *82*, 270–283.
(52) (a) Francl, M. M.; Pietro, W. J.; Hehre, W. J.; Binkley, J. S.; Gordon, M. S.; Defrees, D. J.; Pople, J. A. *J. Chem. Phys.* **1982**, *77*, 3654–3665. (b) Hehre, W. J.; Ditchfield, R.; Pople, J. A. *J. Chem. Phys.* **1972**, *56*, 2257–2261. (c) Hariharan, P. C.; Pople, J. A. *Theor. Chim. Acta* **1973**, *28*, 213–222.
(53) Frisch, M. J.; et al. *Gaussian 09*, revision A.1; Gaussian, Inc.: Wallingford, CT, 2009.
(54) (a) Hehre, W. J.; Stewart, R. F.; Pople, J. A. *J. Chem. Phys.* **1969**, *51*, 2657. (b) Collins, J. B.; Schleyer, P. v. R.; Binkley, J. S.; Pople, J. A. *J. Chem. Phys.* **1976**, *64*, 5142–5151.
(55) Reed, R.; Curtiss, L. A.; Weinhold, F. *Chem. Rev.* **1988**, *88*, 899–926.